Nonlinear Unsteady Potential Flow Calculations for Three-Dimensional Oscillating Wings

W. Geissler*
Deutsche Forschungs- und Versuchsanstalt für Luft- und Raumfahrt e. V., Aerodynamische Versuchsanstalt Göttingen, Göttingen, West Germany

A numerical method has been developed to calculate steady and unsteady pressure distributions on harmonically oscillating three-dimensional wings in incompressible flow. Differing from existing mean-surface theories, in this method the geometric boundary condition is matched on the real wing surface, thus taking into account thickness and camber effects as well as a static mean incidence of the wing. The wake geometry, which is assumed to be known, may be of arbitrary shape. Wing and wake surfaces are represented by a large number of small plane-surface elements each having a constant source sink and doublet distribution of yet unknown strength. The source strengths are determined by solving a large linear system of equations. The doublet strengths are found by applying the Kutta condition at the trailing edge of the wing. Results of the present method are compared with other methods as well as with experimental data.

Nomenclature

x,y,z	= global, body fixed Cartesian coordinate system
ξ,η,ζ	= surface panel coordinates
b	= wing span
S	= wing surface
W	= wake surface
Λ	= aspect ratio, $\Lambda = b^2/S$
l	= wing inner chord length (reference length)
α_s	= static angle of incidence
α'	= oscillation amplitude
t	= time
ω	= frequency
Φ,φ	= velocity potential
u	= induced velocity vector, $u = \text{grad } \varphi$; components: u,v,w
V	= velocity vector of the oscillatory movement
U_∞	= velocity vector of the translatory movement (U_∞ = reference velocity)
w	= resulting velocity vector, $w = u + U_\infty + V$
p	= steady, unsteady pressure
ρ	= density
c_p	= pressure coefficient

Subscripts

s	= steady
i	= unsteady
∞	= reference condition
T	= trailing edge
q	= source distribution
d	= doublet distribution
u,l	= wing upper/lower surface
a	= pitching axis

I. Introduction

SEVERAL numerical methods, based on the acceleration potential[1] or the velocity potential,[2,3] have been developed in recent years for the calculation of unsteady airloads on harmonically oscillating wings. In these cases, the wing is represented by its infinite thin mean surface on which the kinematic boundary condition is applied. This linearization leads to a complete separation of the problem into a steady and an unsteady part.

Received Nov. 30, 1977; revision received May 4, 1978.

Index category: Nonsteady Aerodynamics.

*Research Scientist, Institute of Aeroelasticity.

For the special case of incompressible flow, the governing potential equation is the Laplace equation and, therefore, a complicated potential can be built up by superposition of single parts. It has been shown[4,5] that it is possible to calculate steady and unsteady pressure distributions on oscillating bodies without linearization of the kinematic boundary condition or of the Bernoulli equation. In addition to steady and first harmonic parts, pressures due to the second and higher harmonics can be calculated. However, now a connection exists between steady and unsteady solutions and thus both must be calculated together.

The present method solves the corresponding problem for a wing with arbitrary planform and thickness. The real surface is represented by a source-sink distribution and, in addition, by a doublet distribution, where the latter is emanating from the trailing edge into the wake. The geometry of the wake is assumed to be known. This assumption is a simplification compared to the two-dimensional method of Giesing,[6] who calculates the shape of the wake by an iteration process. The numerical solution process is similar to the method for steady potential flow problems with lift, derived by the method of Hess.[7] Theoretically, it is sufficient to take a doublet distribution alone,[8,9] but the author's experience reveals that this concept leads to numerical difficulties, especially at the wing's trailing edge.

The present method has been applied for the calculation of steady and unsteady pressure distributions on wings with different planforms and with a variety of oscillation modes and frequencies. The influence of finite thickness in the case of an oscillating trailing edge flap was investigated. Boundary-layer corrections were carried out for special cases.

With the introduction of appropriate compressibility corrections, it should be possible to extend the method to compressible subsonic flows.

II. Formulation of the Problem and Boundary Conditions

The configuration considered is given in Fig. 1. The wing geometry is expressed in a global coordinate system x,y,z. The oncoming flow, with the velocity vector U_∞, may be inclined to the x axis by a static mean angle of attack α_s. The oscillatory movement of the wing is carried out about this mean static position. Three different oscillation modes are frequently investigated: 1) plunging oscillations; 2) pitching oscillations about an arbitrary axis which can, for instance, be inclined to the x,z plane; and 3) oscillation of a trailing edge

flap about the flap hingeline. Other, more difficult modes, can be realized without problems.

With the geometries of the wing surface and the wake and with the translatory and oscillatory movements of the configuration, the boundary condition can be specified at arbitrary surface points. The problem then is to find a potential distribution in such a way that the prescribed normal velocities at a surface control point are cancelled by the induced velocity of this potential. After the kinematic boundary condition has been fulfilled, pressures and forces can be calculated by means of Bernoulli's theorem.

The governing equation for the velocity potential is the Laplace equation:

$$\Delta\Phi = 0 \tag{1}$$

Therefore, the arbitrary time-dependent potential can be expressed in terms of steady and unsteady parts by superposition

$$\Phi(x,y,z,t) = \varphi_\infty + \varphi_s + \bar{\varphi}_i \alpha' e^{i\omega t} \tag{2}$$

with α' as the oscillation amplitude. It is shown[5] that in Eq. (2) higher order terms due to the second or higher harmonics can also be taken into account. In the following, it is assumed that the oscillation amplitude α' is sufficiently small to allow for neglecting these terms.

The kinematic boundary condition on the wing surface can now be expressed by:

$$\frac{DS}{Dt} = \frac{\partial S}{\partial t} + (\boldsymbol{u} + \boldsymbol{U}_\infty)\cdot\nabla S = 0 \tag{3}$$

with

$$\boldsymbol{u} = \text{grad}(\varphi_s + \varphi_i), \qquad \boldsymbol{U}_\infty = \text{grad}\ \varphi_\infty$$

If Eq. (3) is divided by $|\nabla S|$, one obtains

$$\frac{\partial \varphi_s}{\partial \zeta} + \frac{\partial \varphi_i}{\partial \zeta} = -\left(\frac{\partial \zeta}{\partial t} + \vec{\zeta} U_\infty\right) \tag{4}$$

with

$$\frac{\nabla S}{|\nabla S|} \equiv \vec{\zeta}$$

as the unit normal vector in a surface point and

$$\frac{1}{|\nabla S|}\frac{\partial S}{\partial t} \equiv \frac{\partial \zeta}{\partial t}$$

The terms on the right-hand side of Eq. (4) are prescribed quantities with ζ as the time-dependent normal displacement of a surface point and $\vec{\zeta} U_\infty$ as the instantaneous normal velocity component of the oncoming flow. The left-hand side of Eq. (4) represents both the steady and unsteady induced normal velocity components of the unknown potential distribution. This unknown potential can now be expressed as the potential of surface singularities of both source and doublet type

$$\varphi_q(x,y,z) = \frac{1}{4\pi}\iint_S \frac{\sigma_q(x',y',z')}{r}\,dS \tag{5}$$

$$\varphi_d(x,y,z) = \frac{1}{4\pi}\iint_S \sigma_d(x',y',z')\frac{\partial}{\partial \zeta'}\left(\frac{1}{r}\right)dS + \frac{1}{4\pi}\iint_W \Delta\varphi_{dw}(x',y',z')\frac{\partial}{\partial \zeta'}\left(\frac{1}{r}\right)dW \tag{6}$$

with S and W as the wing and wake surfaces, respectively. Here r is the distance between the control point $P(x,y,z)$ and the integration point $P'(x',y',z')$, or

$$r = [(x-x')^2 + (y-y')^2 + (z-z')^2]^{1/2} \tag{7}$$

Denoting the outer normal direction at the surface control point by ζ, the differentiation of Eqs. (5) and (6) with respect to ζ gives the corresponding normal velocity components of the source and doublet distributions used for the left-hand side of Eq. (4).

The problem now is to find the unknown source and doublet strengths of Eqs. (5) and (6), matching the boundary condition, Eq. (4). It will be shown that this leads to a system of integral equations which can be solved by numerical means.

III. System of Integral Equations

Both terms on the right-hand side of Eq. (4) can be expressed by steady and unsteady parts

$$\vec{\zeta} U_\infty = U_{\zeta s} + \bar{U}_{\zeta i}\alpha' e^{i\omega^* T} \tag{8a}$$

$$\frac{\partial \zeta}{\partial t} = \bar{V}_\zeta \alpha' e^{i\omega^* T} \tag{8b}$$

with the reduced frequency $\omega^* = \omega \cdot l/U_\infty$ and $T = t \cdot U_\infty / l$.

For the case of pitching oscillations, the terms $U_{\zeta s}$, $\bar{U}_{\zeta i}$, and $\bar{V}_\zeta$ are given in the Appendix. With Eqs. (2) and (8), Eq. (4) can be expressed as:

$$\frac{\partial \varphi_s}{\partial \zeta} + \frac{\partial \bar{\varphi}_i}{\partial \zeta}\alpha' e^{i\omega^* T} = -[U_{\zeta s} + (\bar{V}_\zeta + \bar{U}_{\zeta i})\alpha' e^{i\omega^* T}] \tag{9}$$

Due to the linearity of the problem, Eq. (9) is now split into a system of equations with a steady part

$$\frac{\partial \varphi_s}{\partial \zeta} = -U_{\zeta s} \tag{10a}$$

and an unsteady part

$$\frac{\partial \bar{\varphi}_i}{\partial \zeta} = -(\bar{V}_\zeta + \bar{U}_{\zeta i}) \tag{10b}$$

where the exponential time function in Eq. (10b) is cancelled. For the second or higher harmonics, additional equations can be formulated.

If source and doublet distributions are used, the steady potential φ_s as well as the unsteady potential φ_i are the sum of a source and doublet term

$$\varphi = \varphi_q + \varphi_d \tag{11}$$

Similar to Hess,[7] it is assumed in the first step that the doublet strengths σ_d in φ_d are known. Then, the normal derivatives $\partial\varphi_d/\partial\zeta$ for each steady and unsteady case are transferred to the right-hand side of Eqs. (10a) and (10b)

$$\frac{\partial \varphi_{qs}}{\partial \zeta} = -\left(U_{\zeta s} + \frac{\partial \varphi_{ds}}{\partial \zeta}\right) \tag{12a}$$

$$\frac{\partial \bar{\varphi}_{qi}}{\partial \zeta} = -\left(\bar{V}_\zeta + \bar{U}_{\zeta i} + \frac{\partial \bar{\varphi}_{di}}{\partial \zeta}\right) \tag{12b}$$

Equations (12) are the final integral equations, with the normal derivatives of source and doublet potential

$$\frac{\partial \varphi_q}{\partial \zeta} = \frac{1}{4\pi}\iint_S \sigma_q \frac{\partial}{\partial \zeta}\left(\frac{1}{r}\right)dS \tag{13}$$

$$\frac{\partial \varphi_d}{\partial \zeta} = \frac{1}{4\pi}\iint_S \sigma_d \frac{\partial^2}{\partial\zeta\partial\zeta'}\left(\frac{1}{r}\right)dS + \frac{1}{4\pi}\iint_W \Delta\varphi_{dw}\frac{\partial^2}{\partial\zeta\partial\zeta'}\left(\frac{1}{r}\right)dW \tag{14}$$

where the source term is the same for both steady and unsteady cases; while the influence function of the wake, the second term of Eq. (14), shows considerable differences in both cases. After the integral equations (12), have been solved for the unknown source strengths, the doublet strengths must be calculated by applying the Kutta condition at the trailing edge of the wing.

The numerical solution of the integral equations (12) and their reduction to one linear system of equations will be given in a following section. The calculation of the pressure distribution on the wing surface will be discussed first.

IV. Unsteady Bernoulli Equation

The incompressible time-dependent Bernoulli equation in a body-fixed coordinate system[5] has the form

$$\frac{\partial\Phi}{\partial t} + \frac{w\cdot w}{2} + \frac{p}{\rho} = \frac{(U_\infty + V)^2}{2} + \frac{p_\infty}{\rho} \tag{15}$$

with w as the resulting velocity vector relative to the moving surface. Equation (15) gives the dimensionless pressure coefficient

$$c_p = \frac{p-p_\infty}{\rho/2U_\infty^2} = \frac{(U_\infty+V)^2}{U_\infty^2} - \frac{2}{U_\infty^2}\frac{\partial\Phi}{\partial t} - \frac{w\cdot w}{U_\infty^2} \tag{16}$$

In a ξ,η,ζ surface coordinate system (Fig. 1) the vector product $w\cdot w$ yields

$$w\cdot w = [\vec{\xi}(u+U_\infty+V)]^2 + [\vec{\eta}(u+U_\infty+V)]^2 \tag{17}$$

If this product is calculated, and if higher order terms are again neglected, then the pressure coefficients can be split into a steady part

$$c_{ps} = 1 - (1/U_\infty^2)[(u_s+U_{\xi s})^2 + (v_s+U_{\eta s})^2] \tag{18}$$

and an unsteady part

$$c_{pi} = (2/U_\infty^2)\{[U_{\xi s}\bar{V}_\xi + U_{\eta s}\bar{V}_\eta + U_{\zeta s}\bar{V}_\zeta] - [i\omega^*\bar{\varphi}_i + (u_s+U_{\xi s})(\bar{u}_i + \bar{U}_{\xi i} + \bar{V}_\xi) + (v_s+U_{\eta s})(\bar{v}_i + \bar{U}_{\eta i} + \bar{V}_\eta)]\}\alpha' e^{i\omega^* T} \tag{19}$$

It should be mentioned again that neglecting higher order terms is not necessary. If it is not done, it would lead to higher order pressure coefficients due to $\alpha'^2 e^{2i\omega^* T}$ etc.[5] This is, of course, only meaningful if the boundary conditions and corresponding integral equations have been solved up to the same degree of accuracy in the previous step.

V. Kutta Condition

The wake behind the wing is a stream surface. Thus, the pressure difference between two points directly above and below this surface must be zero. From Eq. (15) one obtains

$$\frac{\partial(\Phi_u - \Phi_l)}{\partial t} + \frac{(w\cdot w)_u - (w\cdot w)_l}{2} = 0 \tag{20}$$

with

$$\frac{\partial(\Phi_u - \Phi_l)}{\partial t} = i\omega^*\frac{U_\infty}{l}\Delta\bar{\varphi}_i\alpha' e^{i\omega^* T} \tag{21}$$

and $\Delta\bar{\varphi}_i$ as the unsteady potential jump in the wake. The resulting velocity vector in the wake relative to the moving system has the magnitude

$$w = (U_{\infty s} + \text{grad}\,\varphi_s) + (\bar{U}_{\infty i} + \bar{V} + \text{grad}\,\bar{\varphi}_i)\alpha' e^{i\omega^* T} \tag{22}$$

Substituting Eqs. (21) and (22) into Eq. (20) and assuming that the steady pressure difference in the wake is zero, independently of the unsteady pressure difference yields, for the steady part,

$$\text{grad}(\Delta\varphi_s) = 0, \quad \Delta\varphi_s = \text{const} = (\Delta\varphi_s)_T \tag{23}$$

Thus, in a steady flow, the potential jump in the wake at a special spanwise position is of a constant value, which equals the potential jump at the trailing edge. Using this steady condition, the unsteady part of the problem can now be formulated. It is assumed that

$$(U_\infty + \text{grad}\,\varphi_s) \approx sU_\infty$$

with s as the unit tangent vector of the wake in streamwise direction. The unsteady potential jump $\Delta\varphi_i$ in the wake can also be related to its value at the trailing edge by the formula

$$(\Delta\bar{\varphi}_i)_W = (\Delta\bar{\varphi}_i)_T \cdot e^{-i\omega^*(s-s_T)} \tag{24}$$

with s_T as the position of the trailing edge. Equation (24) has to be substituted into Eqs. (6) and (14) for the potential of a doublet distribution and its derivative, thus leading to some rather complicated unsteady wake influence functions in the unsteady case.

After the doublet distributions in the wake of both steady and unsteady flows have been specified, the doublet strengths determining the overall lift of a wing section must be calculated in a satisfactory manner. For numerical considerations, it is very difficult to apply the Kutta condition directly at the trailing edge. Uncertainties occur if the Kutta condition is applied at a wake point a small distance downstream of the trailing edge.

In the present method, the zero pressure difference is determined at the two points on the wing upper and lower surface adjacent to the trailing edge. This condition is fulfilled for both steady and unsteady cases separately. The corresponding numerical procedure is described in the next section.

VI. Discretization and Numerical Solution Procedure

To solve the integral equations (12) for the unknown source strengths σ_q in Eq. (13), a panel-type method was applied. The surface of the wing is represented by a large number of small quadrilateral surface elements (Fig. 1) which are arranged in streamwise sections. These sections are extended into the wake; thus forming semi-infinite wake strips.

Both source and doublet strengths are assumed to be constant for each surface element. In the wake, the doublet strengths are related to their local trailing edge values by Eqs. (23) and (24).

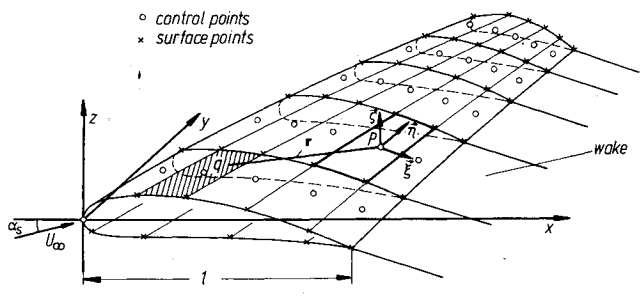

Fig. 1 Wing geometry, panel arrangement.

With this discretization process, the surface integrals for the potentials, Eqs. (5) and (6), and their normal derivatives, Eqs. (13) and (14), are reduced in the usual way to a sum of integrals over single plane panel surfaces; each with constant singularity strengths.

Reference 10 shows how these aerodynamic influence functions can be treated numerically. The surface integrals of the source potential and its derivatives can be reduced to simple line integrals along the perimeter of a surface element as described by Hess.[7] In a similar way, one can reduce the doublet surface integrals to line integrals which can also be solved analytically.

Substituting Eq. (24) into Eqs. (6) and (14), one obtains for the unsteady wake integrals the expressions

$$\bar{\varphi}_{diw} = \frac{(\Delta\bar{\varphi}_i)_T}{4\pi} \int\int_{\Delta W} e^{-i\omega^*(s-s_T)} \frac{\partial}{\partial\zeta'}\left(\frac{1}{r}\right) \mathrm{d}W \tag{25}$$

$$\frac{\partial\bar{\varphi}_{diw}}{\partial\zeta} = \frac{(\Delta\bar{\varphi}_i)_T}{4\pi} \int\int_{\Delta W} e^{-i\omega^*(s-s_T)} \frac{\partial^2}{\partial\zeta\partial\zeta'}\left(\frac{1}{r}\right) \mathrm{d}W \tag{26}$$

where ΔW is the surface of a semi-infinite wake strip.

The spanwise integration of Eqs. (25) and (26) can be carried out analytically. The remaining semi-infinite integral of the form

$$J = \int_0^\infty e^{i\nu s} f(s)\,\mathrm{d}s \tag{27}$$

can be solved as described in Ref. 3. With $\tau = \pi/|\nu|$, Eq. (27) is transformed into

$$J = \left\{\int_0^\tau + \int_0^{2\tau} + \int_0^{3\tau} + \ldots e^{i\nu s} f(s)\,\mathrm{d}s\right\} \tag{28}$$

Due to the periodicity of the function $e^{i\nu(s+n\tau)}$ $(n=1,2,\ldots)$, Eq. (28) can be written as an integral between finite boundaries, with an infinite series in its integrand, as

$$J = \int_0^\tau e^{i\nu s}\left(f(s) - f(s+\tau) + f(s+2\tau) - + \ldots\right)\mathrm{d}s \tag{29}$$

The infinite series in Eq. (29) is evaluated directly up to the term $n=N$. The remaining terms are approximated by a geometric series. The integral in Eq. (29) is then calculated by Simpson's rule.

No difficulties are encountered in the evaluation of the steady wake integrals. The corresponding expressions are identical to the surface integrals, and thus can be calculated analytically.

It is obvious that the left-hand sides of both steady and unsteady integral equations, Eqs. (12), are identical. Thus, the solution of this system is further simplified because only one linear system of equations must be solved with a corresponding number of right-hand sides. These right-hand sides are now formed by steady and unsteady parts, thus expressing the prescribed normal velocities of the translatory and oscillatory movements of the wing and the steady and unsteady induced normal velocities of the doublet system, respectively.

Special treatment is necessary for the chordwise and spanwise doublet distributions on the wing. In chordwise directions, prescribed linearly varying doublet strengths are assumed. However, this linear dependency is approximated by a step function of constant strength for each panel. The doublet variation in spanwise direction is also approximated by a step function. This leads to constant doublet strengths within each surface panel, that is, analogous to concentrated vortices around the perimeter of the panel.

The overall doublet strengths of each lifting-wing section are still unknown and must be calculated by the application of the Kutta condition at the trailing edge, as has been previously mentioned. As in Ref. 7, the normal induced velocities of the doublet distribution are expressed by a sum of the influence of all N wing sections including the corresponding wake strips. Thus, the number of right-hand sides of the linear system of equations is now $N+1$ for the steady part and $N+1$ for the unsteady part; which gives the total number of $2(N+1)$ solution vectors σ_q. For the solution of the linear system of equations, the overall doublet strengths are set equal to unity. Then, these vectors are calculated separately for the steady and unsteady parts of the problem, with the condition that the pressure difference between two control points on the wing surface adjacent to the trailing edge must be zero. In the steady case, this condition leads to a quadratic system of equations and in the unsteady case to a linear system of equations for these unknown vectors.[10] After these systems have been solved, the steady and unsteady pressures can be calculated using Eqs. (18) and (19) and taking into account all induced velocity vectors of both source and doublet distributions.

VII. Discussion of Results

Rectangular Wing with Incidence

A systematic investigation of steady and unsteady airloads on an oscillating rectangular wing with a NACA 0012 airfoil has been given in Ref. 10. The results of the present method were also compared with corresponding experimental data.[11] The experimental investigation was carried out for the low-speed flow regime for a variety of static mean incidences, oscillation frequencies, and amplitudes. For the case of pitching oscillations about the wing quarter chord-axis, typical calculated and measured results were compared, as shown in the following figures.

Figure 2 shows the steady pressure distributions c_{ps} for three different spanwise sections of the wing at $y/l = 0.55/0.815/0.962$ for $\alpha_s = 6$ deg. Inboard of more than 80% of the wing half-span, the results of the potential theory show only small differences when compared with experiment. The outer section at 96.2% of the wing half-span shows the expected influences of the wing tip vortex, which occurs mainly on the upper surface of the wing. A similar behavior can be observed in the unsteady cases.

Figure 3 shows unsteady pressure distributions for zero mean incidence $\alpha_s = 0$. In this special case, the results can be compared with mean-surface theories. The real parts of the pressure distributions show considerable differences of both linear and nonlinear results. In the front part of the sections, the pressure of the linearized method is too low but has a steep gradient at the leading edge due to the square root singularity there. At the aft portion, the linearized pressure is slightly larger in comparison with the nonlinearized values. The imaginary parts c_{pi}'' show only small differences between the two theoretical concepts. A similar behavior has been observed for all other oscillation frequencies which have been investigated for this configuration.

Figure 4 gives the corresponding results for the case of a static mean incidence $\alpha_s = 6$ deg. As in the steady case, the correspondence between theoretical and experimental results is quite good for the two inner sections, whereas the real parts of the unsteady pressure distributions for the outer section show the same differences and tendencies as in the steady case (Fig. 2). It is noteworthy that the imaginary parts in this outer region do not show any irregularities.

The results discussed so far clearly show the differences and the agreement of the present nonlinear method in comparison with mean surface theories. The results, however, show also the limitations of potential theory and so postulate where viscous effects are no longer negligible; as the very tip region of a wing with a tip vortex formation.

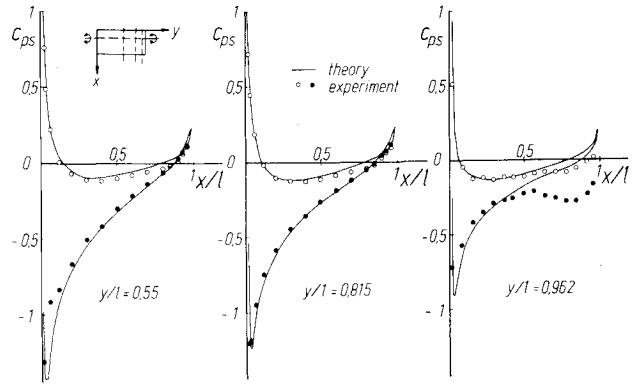

Fig. 2 Steady pressure distributions for a rectangular wing, $\Lambda = 4$, $\alpha_s = 6$ deg.

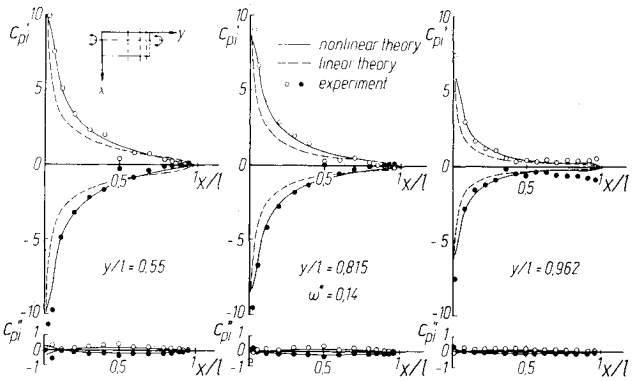

Fig. 3 Unsteady pressure distributions for a rectangular wing, $\Lambda = 4$, $\alpha_s = 0$ deg, $\omega^* = 0.14$.

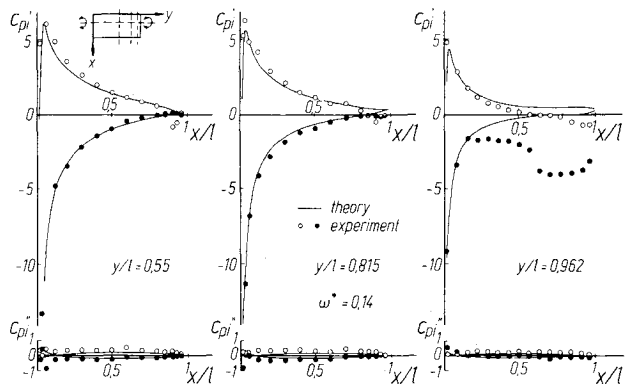

Fig. 4 Unsteady pressure distributions for a rectangular wing, $\Lambda = 4$, $\alpha_s = 6$ deg, $\omega^* = 0.14$.

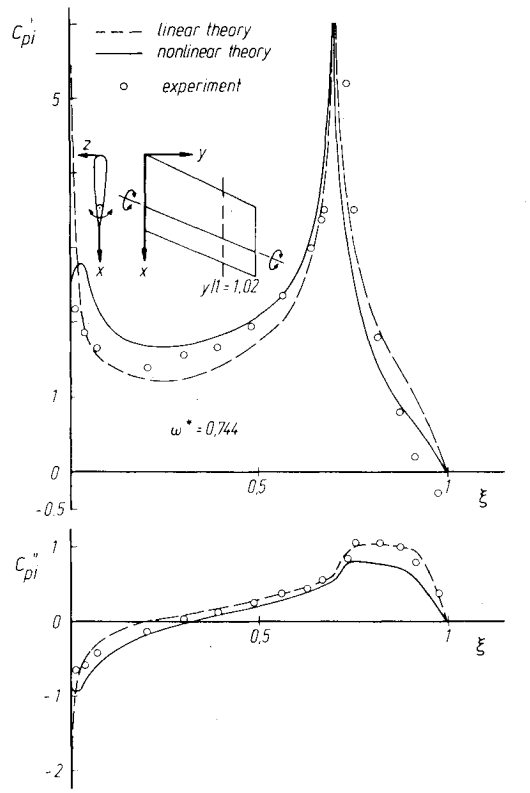

Fig. 5 Unsteady pressure distributions for a swept wing with control surface, $\Lambda = 2.94$, $\alpha_s = 0$ deg, $\omega^* = 0.744$.

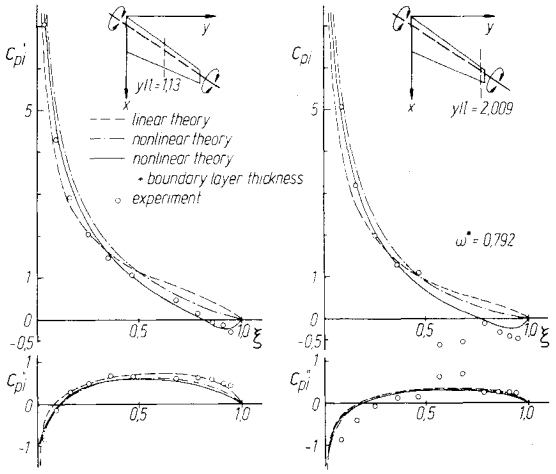

Fig. 6 Unsteady pressure distributions for a swept tapered wing, $\Lambda = 2$, $\alpha_s = 0$ deg, $\omega^* = 0.792$, boundary-layer corrections.

Swept-Wing with Trailing Edge Flap

Another systematic investigation of the influence of finite thickness on unsteady airloads has been carried out for a swept wing with a trailing edge flap. Typical results are given in Fig. 5 for a wing with a leading and trailing edge sweep angle of 25 deg. Again, a NACA 0012 section was investigated. Theoretical results are given again for both linearized and nonlinearized methods. Experimental data[12] are also included in Fig. 5. The differences between the two theoretical concepts are similar when compared to the rectangular wing case. The experimental data show larger differences in the region adjacent to the flap hingeline, which can be interpreted as the influence of a small gap between wing and control surfaces in the experimental case. This gap was not included in the calculation process. To analyze the correct effect of a gap between wing and flap, viscous effects have to be taken into consideration. The first step in accounting for boundary-layer effects on the unsteady pressure distributions is described in the next section.

Boundary-Layer Correction

Figure 6 shows unsteady pressure distributions at two sections of a swept tapered wing of $\Lambda = 2$, with 37 deg leading edge sweep angle and 24 deg trailing edge sweep. The wing undergoes pitching oscillations about the quarter-chord axis. The results in Fig. 6 are given only for the upper surface of the wing at two spanwise sections, $y/l = 1.13$ and $y/l = 2.01$, and for the zero mean incidence case. The wing has a NACA 0010 airfoil. Three different curves are included in Fig. 6:

1) Results from the mean surface theory.[3]

2) Results of the present nonlinear analysis without any boundary layer corrections.

3) Results of the present nonlinear analysis including the effect of the boundary layer displacement-thickness.

For the third step, a two-dimensional, boundary-layer calculation[13] was carried out for the different wing sections, taking into account the three-dimensional steady pressure distributions of the second step. The boundary-layer displacement thickness, obtained from the boundary-layer calculation, was then added to the profile coordinates, thus forming a thickened profile.

The procedure of adding the boundary-layer displacement thickness has been simplified by taking only the data from one section in the midspan region and then adding these data to all other sections. The results shown in Fig. 6 were also compared with detailed experimental data.[14]

It is interesting to observe in the plots the results of the different calculations. The simple boundary-layer correction already gives a considerable reduction of the real part of the pressure distribution when compared with the case without boundary layer. The experimental data are thus well predicted by the corrected pressures. In the outer aft portion of the wing (section $y/l=2.01$), a boundary-layer separation can be observed which has an influence on both the real and the imaginary pressure parts.

VIII. Conclusions

A numerical method has been presented for the calculation of unsteady airloads on oscillating three-dimensional wings of arbitrary planform and thickness. The kinematic boundary condition is fulfilled on the real wing surface. It appears that a static mean angle of incidence can be taken into account. Numerous results with the presented method have been compared with existing mean surface theories as well as with experimental data. The method has also been applied to the case of an oscillating control surface. A simple boundary-layer correction, taking into account the boundary-layer displacement thickness of the steady flow, has been investigated.

The results indicate the significance of the effects of the wing thickness and steady mean angle of incidence. The boundary-layer correction shows clearly the main effects of viscosity, especially in the trailing edge region of the wing. These effects already occur in the zero mean incidence case. More complex viscous effects, such as separation, wing tip vortex, and flow through a gap between wing and control surface, need further detailed investigation; where the inviscid results can serve as a useful tool.

Appendix: Calculation of Velocity Components of V and U_∞ in a Body-Fixed Frame of Reference for the Case of Pitching Oscillations

The surface panel coordinate system ξ,η,ζ (Fig. 1) has the following components in the global body system (unit vectors i,j,k)

$$\vec{\xi}=\xi_x\cdot i+\xi_z\cdot k \quad \text{(streamwise direction)}$$
$$\vec{\eta}=\eta_x\cdot i+\eta_y\cdot j+\eta_z\cdot k \quad (\vec{\eta}=\vec{\zeta}\times\vec{\xi})$$
$$\vec{\zeta}=\zeta_x\cdot i+\zeta_y\cdot j+\zeta_z\cdot k \quad (\vec{\zeta}=d_1\times d_2) \tag{A1}$$

with d_1 and d_2 as the unit diagonal vectors in the element plane.

In the case of pitching oscillations about an axis perpendicular to the x,z plane, the velocity vector of a surface point (x,y,z) is given by:

$$V=i\omega^*[-(z-z_a)i+(x-x_a)k]\alpha' e^{i\omega^* T} \tag{A2}$$

(x_a,z_a = location of the pitching axis) with the components V_ξ, V_η, V_ζ in element coordinates.

The instantaneous angle of incidence for pitching oscillations about a static mean position is:

$$\alpha=\alpha_s+\alpha' e^{i\omega^* T} \tag{A3}$$

Then, the velocity components at a surface point due to the translatory movement of the wing has the components in a body-fixed frame of reference

$$U_\infty=U_\infty(\cos\alpha\cdot i+\sin\alpha\cdot k) \tag{A4}$$

Substituting Eq. (A3) into (A4) and developing the terms $\sin\alpha$ and $\cos\alpha$ in series

$$\sin\alpha=\sin(\alpha_s+\alpha' e^{i\omega^* T})\approx\sin\alpha_s+\cos\alpha_s\alpha' e^{i\omega^* T}$$
$$\cos\alpha=\cos(\alpha_s+\alpha' e^{i\omega^* T})\approx\cos\alpha_s-\sin\alpha_s\alpha' e^{i\omega^* T} \tag{A5}$$

where only the linear unsteady term has been taken into account; U_∞ [(Eq. (A4)] can be expressed by steady parts

$$U_s=\cos\alpha_s\cdot i+\sin\alpha_s\cdot k \tag{A6}$$

and unsteady parts

$$U_i=(-\sin\alpha_s\cdot i+\cos\alpha_s\cdot k)\alpha' e^{i\omega^* T} \tag{A7}$$

with the components U_ξ, U_η, U_ζ in element coordinates.

The ζ components of Eqs. (A2), (A6), and (A7) are used for the right-hand sides of the integral equations, Eqs. (12). All steady and unsteady terms enter Eqs. (18) and (19) to calculate the corresponding pressure coefficients.

References

[1] Albano, E. and Rodden, W. P., "A Doublet-Lattice-Method for Calculating Lift Distributions on Oscillating Surfaces in Subsonic Flow," *AIAA Journal*, Vol. 7, Feb. 1969, pp. 279-285.

[2] Jones, W. P. and Moore, J. A., "Simplified Aerodynamic Theory of Oscillating Thin Surfaces in Subsonic Flow," *AIAA Journal*, Vol. 11, Sept. 1973, pp. 1305-1309.

[3] Geissler, W., "Ein numerisches Verfahren zur Berechnung der instationären aerodynamischen Druckverteilung der harmonisch schwingenden Tragfläche mit Ruder in Unterschallströmung. Part I: Theorie und Ergebnisse für inkompressible Strömung," Deutsche Luft- und Raumfahrt Forschungsbericht DLR-FB 75-37, 1975." Part II: Theorie und Ergebnisse für kompressible Strömung," Deutsche Luft- und Raumfahrt Forschungsbericht DLR-FB 77-15, 1977.

[4] Morino, L., et al., "Steady and Oscillatory Subsonic and Supersonic Aerodynamics around Complex Configurations," *AIAA Journal*, Vol. 13, March 1975, pp. 368-374.

[5] Geissler, W., "Berechnung der Druckverteilung an harmonisch oszillierenden dicken Rümpfen in inkompressibler Strömung," Deutsche Luft- und Raumfahrt Forschungsbericht DLR-FB 76-48, 1976.

[6] Giesing, J. P., "Nonlinear Two-Dimensional Unsteady Potential Flow with Lift," *Journal of Aircraft*, Vol. 5, No. 2, March-April 1968, pp. 135-143.

[7] Hess, J., "The Problem of Three-Dimensional Lifting Potential Flow and its Solution by Means of Surface Singularity Distributions," Computer Methods in Applied Mechanics and Engineering 4, 1974, pp. 283-319.

[8] Djojodihardjo, R. H. and Widnall, S. E., "A Numerical Method for the Calculation of Nonlinear Unsteady Lifting Potential Flow Problems," *AIAA Journal*, Vol. 7, Oct. 1969, pp. 2001-2009.

[9] Summa, J. M., "Unsteady Potential Flow about Wings and Rotors Started Impulsively from Rest," Symposium on Unsteady Aerodynamics, R. B. Kinney, ed., Univ. of Arizona, Tucson, 1975, pp. 741-767.

[10]Geissler, W., "Berechnung der Druckverteilung an oszillierenden dreidimensionalen Tragflächen mit endlicher Dicke in inkompressibler Strömung," DFVLR-AVA-Internal Rept. 253-76 J 05, 1976.

[11]Triebstein, H., "Instationäre Druckverteilungsmessungen an angestellten Rotorblattspitzen in inkompressibler Strömung," Deutsche Luft- und Raumfahrt Forschungsbericht DLR-FB 76-42, 1976.

[12]Försching, H., Triebstein, H., and Wagener, J., "Pressure Measurements on a Harmonically Oscillating Swept Wing with Two Control Surfaces in Incompressible Flow," Deutsche Luft- und Raumfahrt Forschungsbericht DLR-FB 70-49, 1970.

[13]Rotta, J. C., "FORTRAN IV-Rechenprogramm für Grenzschichten bei kompressiblen, ebenen und rotationssymmetrischen Strömungen," Deutsche Luft- und Raumfahrt Forschungsbericht DLR-FB 71-51, 1971.

[14]Triebstein, H., "Instationäre Druckverteilungsmessungen an Flügel-Aussenlastkombinationen in inkompressibler Strömung," Deutsche Luft- und Raumfahrt Forschungsbericht DLR-FB 77-12, 1977.